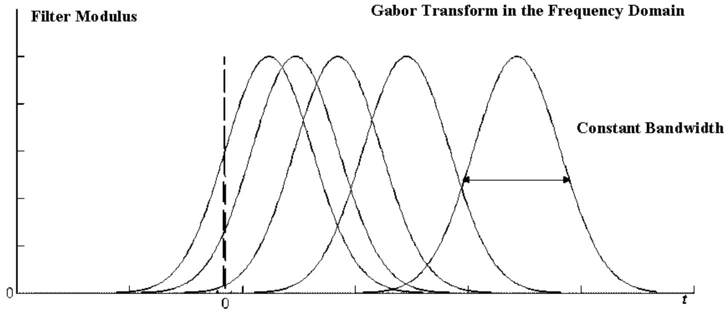

(a)

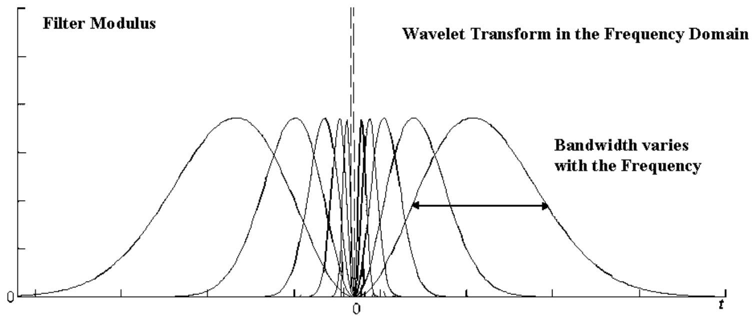

(b)

Figure 7.1: *The interpretation of the Gabor and wavelet transforms as filters illustrates that in the former the filter bandwidth remains the same for different frequencies, while the latter applies larger filters for higher frequencies.*

<u>To probe further</u>: *The Continuous and the Discrete Wavelet Transforms*

Among the important developments that followed from the wavelet theory, it is worth noting its connection to several related developments, such as the *multiresolution analysis*, developed in the works of Stéphane Mallat and Yves Meyer [Mallat, 1989; Meyer, 1993]; sub-band filter banks; and the orthonormal wavelets developed by Ingrid Daubechies (a former PhD student of Grossmann) [Daubechies, 1992]. These issues, related to the *discrete wavelet transform*, have been successfully applied to many problems of signal coding, compression and transmission, among others. Some comments about the continuous and the discrete wavelet transform are given in the following.

Firstly, what are the main differences between the continuous and the discrete wavelet transforms? This is a difficult and possibly tricky question to answer, mainly because both approaches include a wide and versatile set of

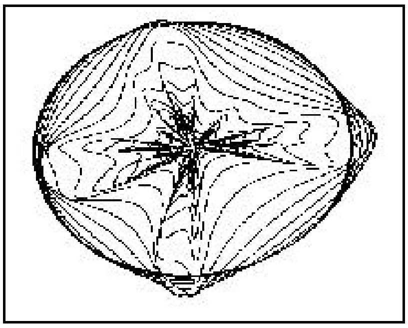

Figure 7.7: *A morphogram. (Adapted from R.M. Cesar Jr. and L. da F. Costa, Application and Assessment of Multiscale Bending Energy for Morphometric Characterization of Neural Cells, Review of Scientific Instruments, 68(5): 2177-2186 , May 1997. Copyright 1997, American Institute of Physics with permission.)*

Note: ***Different Approaches to Shrinking Prevention***

It is important to note that shrinking does not affect all the contour points in the same way, being more accentuated near high curvature points. In fact, there are some techniques that attempt to account for shrinking prevention (e.g. [Mokhtarian and Mackworth, 1992] with basis on the technique developed by [Lowe, 1989]). This section has discussed some simpler approaches that can be applied without substantial numerical errors and are suitable for many practical situations. Further references on this subject can be found in [Marshall, 1989; Oliensis, 1993; Sapiro and Tannenbaum, 1995]. In the case of analysis over small spatial scales, the shrinking effect can naturally be avoided by considering the factor (i.e. the sampling interval) implied by the numerical integration of the Fourier transform [Estrozi et al., 2000].

7.2.5 The Curvegram

The normalized multiscale expressions of $\dot{u}(t,a)$ and $\ddot{u}(t,a)$ defined in the previous sections, together with complex curvature expression of $k(t)$ given by Equation (7.7), allow the definition of the multiscale curvature description, or *curvegram* of $u(t)$ as

$$k(t,a) = \frac{-\operatorname{Im}\left\{\dot{u}(t,a)\,\ddot{u}^*(t,a)\right\}}{\left|\dot{u}(t,a)\right|^3} \tag{7.9}$$

The algorithm below summarizes the curvegram generation by using the aforementioned Fourier properties and perimeter normalization. In fact, this algorithm calculates the curvature for a given fixed scale a. In order to obtain

Because in practice all maxima crests start at the minimum scale $a_0 = a_{min}$, the relevance measure can be defined as:

$$f(L_v) = \log a_1$$

It is important to note that the lifetime criterion is independent of the scale parameter discretization, being easy and fast to calculate. The algorithm has been tested on real images, and its ability to correctly identify the *perceptually important contour points* is illustrated by the following examples. Figure 7.20(a) presents a pliers silhouette, while the vertical skeletons of the corresponding w-representation, before and after the relevance measure-based thresholding operation, are shown in Figure 7.20(b). The dominant points associated with the left vertical maxima lines after thresholding are shown marked with "*" in Figure 7.21(a).

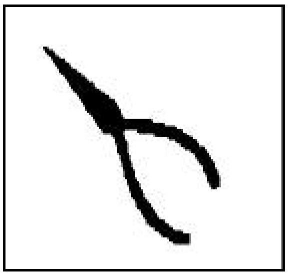

(a)

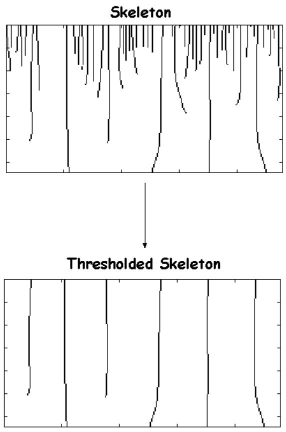

(b)

Figure 7.20: *Pliers shape (a) and wavelet vertical skeletons before and after the relevance thresholding (b).(Reprinted from Signal Processing, 62(3), J.-P. Antoine, D. Barache, R.M. Cesar Jr., L. da F. Costa, Shape characterization with the wavelet transform, 265-290, Copyright (1997), with permission from Elsevier Science.)*

The same procedure has been applied to the fork shape of Figure 7.21(b), where the respective results are presented. Finally, Figure 7.21(c) presents the result with the two shapes superposed and affine transformed (the shapes have been stretched along the x-axis). The additionally detected dominant points correspond to concavities due to the intersection of two surfaces, an important feature for visual perception [Richards et al., 1986].